A Reflector Diffusion Coefficient Correction Method for Pin-wise Diffusion Calculation of PWR Cores

Woo Jin Lee[a], Sung Hyun Cho[a], Ser Gi Hong[a*] and Jooil Yoon[b*]

[a]*Department of Nuclear Engineering, Hanyang University, 222 Wangshimni-ro, Seongdong-gu, Seoul, 04763, Korea*
[b]*KEPCO International Nuclear Graduate School, 658-91 Haemaji-ro, Seosaeng-myeon, Ulju-gun, Ulsan, 45014, Korea*
**Corresponding author. E-mail address: hongsergi@hanyang.ac.kr, jiyoon@kings.ac.kr*

Keywords : Pin-wise core calculation, Reflector diffusion coefficient correction, SPH factor

1. Introduction

As modern core designs such as the soluble-boron-free (SBF) i-SMR [1] rely on large numbers of burnable absorber rods and control rods (CR) for reactivity control, pin-wise core calculation has drawn attention. It uses pin-homogenized group constants (PHGC) directly, removing the pin power reconstruction step and its errors while improving accuracy in these strongly heterogeneous regions.

Pin-wise core calculation requires the equivalence parameters to reproduce the reference solution. The super-homogenization (SPH) factor [2], defined as the ratio of the heterogeneous to homogeneous average fluxes, preserves the reaction rate of each pin cell, and the correction is absorbed into the PHGCs so that no additional storage is needed. With the SPH factor applied, a finite-difference method (FDM) diffusion solver can reproduce the reference transport solution well [3], [4].

A small residual error nevertheless remains in the power distribution. One factor for this residual error is the diffusion coefficient (D) near the fuel assembly (FA)–reflector boundary. In the FDM formulation, the surface current (J) is determined by the coupling of the FA and reflector D, and this current governs the leakage into the reflector. Neither side, however, gives D accurately: the D of FA comes from a single-FA lattice calculation with the $J = 0$ conditions, while on the reflector side the strongly anisotropic angular flux weakens the P_1 assumption. The SPH factor is applied to both regions, but it preserves only the reaction rate, so this error is not fully removed.

The objective of this study is to reduce this residual error by correcting D near the FA–reflector boundary so that the surface current matches the reference one, $J^{hom} = J^{het}$. It is noted that the D of the FA must be kept fixed to follow the two-step scheme. The correction is therefore placed entirely on the reflector side, applied to the SPH-corrected D through a factor γ during the generation of the reflector PHGC. The factor is obtained practically in a closed form, because every quantity other than γ is already available from the converged SPH solution and the reference calculation. The method therefore requires no change to the core solver.

The PHGCs were generated with DeCART2D [5] and the pin-wise diffusion calculations with SPHINCS [6]. For the APR1400, OPR1000, and i-SMR 2D cores, three SPHINCS solutions — with reflector PHGCs without SPH, with SPH, and with SPH plus the D correction — were compared against the reference DeCART2D solution in terms of pin- and FA-wise power distributions.

2. Methodology

Fig. 1 shows the heterogeneous FA–reflector geometry from DeCART2D (top right), the homogenized geometry obtained after pin-wise homogenization and the SPH iteration (bottom right), and the corresponding 1D FDM discretization at the interface (left). Although the core geometry is 2D, the problem is reduced to 1D here, and only the surface current normal to the FA–reflector interface is treated, as shown in the 1D schematic on the left of Fig. 1.

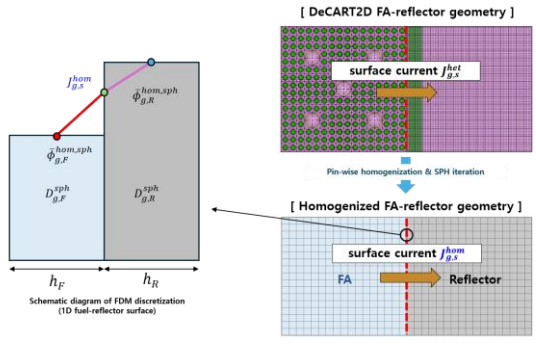


Fig. 1. Heterogeneous (top right) and homogenized (bottom right) FA–reflector geometries, and the 1D FDM discretization at the interface (left).

With this 1D discretization, the current between the two adjacent pin cells is expressed by their diffusion coefficients and average fluxes as in Eq. (1), evaluated from the converged SPH solution of the reference FA–reflector geometry.

$$J_{g,s}^{hom} = -2\frac{\frac{D_{g,F}^{sph}D_{g,R}^{sph}}{h_F \quad h_R}}{\frac{D_{g,F}^{sph}}{h_F}+\frac{D_{g,R}^{sph}}{h_R}}\left(\bar{\phi}_{g,R}^{hom,sph} - \bar{\phi}_{g,F}^{hom,sph}\right), \qquad (1)$$

where $J_{g,s}^{hom}$ is the homogeneous surface current of group g at surface s, $D_{g,F}^{sph}$ and $D_{g,R}^{sph}$ are the SPH-corrected diffusion coefficients of the fuel and reflector pin cells, $\bar{\phi}_{g,F}^{hom,sph}$ and $\bar{\phi}_{g,R}^{hom,sph}$ are the corresponding SPH-corrected average fluxes, and h_F and h_R are the pin cell side lengths.

This homogeneous surface current was then compared with the reference current at each FA–reflector interface, taking the fast group as an example. As Fig. 2 shows, it falls below the reference at every interface without the SPH factor. The SPH factor removes most of this gap and reduces the RMS deviation from 7.0 % to 2.9 %. A fast-group leakage bias nevertheless persists at every interface, since the SPH factor constrains the reaction rate rather than the surface current. The bias is small, yet it acts in the same direction everywhere and can accumulate near the reflector to shift the power distribution.

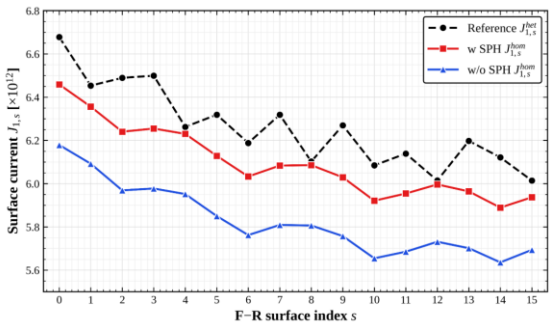


Fig. 2. Comparison of fast-group surface current along the FA-reflector interface

Based on this observation, this study corrects the reflector D in the FA–reflector geometry so that the homogeneous surface current matches the reference one, $J^{\text{hom}} = J^{\text{het}}$ in every energy group. To achieve this, a factor γ multiplying the SPH-corrected reflector D is introduced and determined from the current-matching condition at each interface.

Since modifying the D of FA would break the two-step scheme, the correction is placed entirely in the reflector PHGC generation step. The core calculation then combines the D of FA, generated under the $J = 0$ condition, with the corrected reflector D. Since the matching condition is imposed in the FA–reflector geometry (reference environment) rather than in the core calculation, γ constitutes an approximate correction rather than an exact one.

The reflector nodes are of three types: RE (one FA side), RC (two FA sides at a corner), and RX (no FA side). Within a node, however, the number of FA–reflector interfaces differ from one pin cell to another, and the derivation of γ depends on this number, as presented below.

a) Single FA–reflector interface per pin cell

Fig. 3 shows the single-interface reflector cells, which face one FA–reflector interface, in the RE, RX, and RC regions.

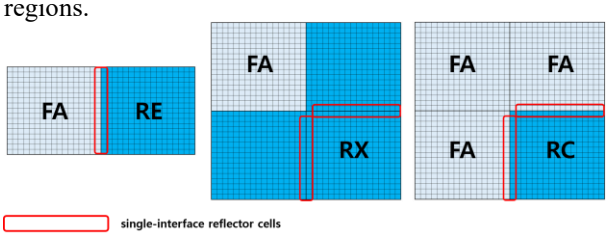


Fig. 3. Single-interface reflector cells (red) in the RE, RX, and RC regions.

The homogeneous surface current at surface s can be obtained from the FDM discretization. Multiplying the reflector-side $D_{g,R}^{sph}$ by the correction factor $\gamma_{g,R}$ and imposing the current-matching condition $J_{g,s}^{hom} = J_{g,s}^{het}$ gives

$$J_{g,s}^{hom} = -\frac{2\gamma_{g,R}\frac{D_{g,R}^{sph}}{h_R}\frac{D_{g,F}^{sph}}{h_F}}{\frac{D_{g,F}^{sph}}{h_F}+\gamma_{g,R}\frac{D_{g,R}^{sph}}{h_R}}\left(\bar{\phi}_{g,R}^{hom,sph}-\bar{\phi}_{g,F}^{hom,sph}\right) = J_{g,s}^{het}. \quad (2)$$

Since all quantities in Eq. (2) except $\gamma_{g,R}$ are known from the SPH-converged solution and the reference current $J_{g,s}^{het}$, the equation can be solved directly for $\gamma_{g,R}$, yielding the closed-form expression as follows:

$$\gamma_{g,R} = \frac{J_{g,s}^{het}\frac{D_{g,F}^{sph}}{h_F}}{\frac{D_{g,R}^{sph}}{h_R}\left[2\frac{D_{g,F}^{sph}}{h_F}\left(\bar{\phi}_{g,R}^{hom,sph}-\bar{\phi}_{g,F}^{hom,sph}\right)-J_{g,s}^{het}\right]}. \quad (3)$$

Applying $\gamma_{g,R}$ to the reflector D enforces $J_{g,s}^{hom} = J_{g,s}^{het}$ at the interface, so that the homogeneous calculation reproduces the reference surface current. Since $\gamma_{g,R}$ is determined in the reference environment, however, it may not exactly preserve the surface current in the actual core calculation, but it modifies the reflector leakage and thereby influences the power distribution.

b) Two adjacent FA–reflector interfaces per pin cell

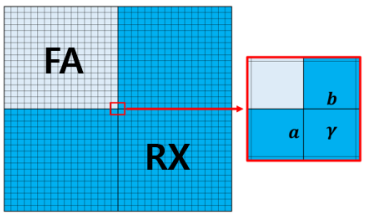


Fig. 4. Two-interface reflector cells (red) in the RX

For a reflector pin cell located at a corner, such as in the RX reflector shown in Fig. 4, the cell faces two adjacent FA–reflector interfaces a and b. In this pin cell,

a single correction factor γ is applied so that the sum of the two homogeneous interface currents matches the sum of the corresponding reference currents, as given in Eq. (4):

$$J_{g,a}^{hom}(\gamma) + J_{g,b}^{hom}(\gamma) = J_{g,a}^{het} + J_{g,b}^{het} \equiv J. \quad (4)$$

Substituting the FDM expression for each surface current and rearranging, Eq. (4) becomes a quadratic equation in γ, whose positive root gives a single γ for the corner pin cell. The same treatment applies to the corner pin cell of the RC reflector.

However, since γ_g is defined only at the reflector boundary of pin cell, it cannot be assigned individually to every reflector pin cell. As an approximation, a single representative value $\bar{\gamma}_g$ is defined for each reflector by taking the flux–volume–weighted average of γ_g over all FA–reflector interfaces belonging to that reflector, as given in Eq. (5):

$$\bar{\gamma}_g = \frac{\sum_{i\in\partial R} \bar{\phi}_{g,i} V_i D_{g,i}^{sph} \gamma_{g,i}}{\sum_{i\in\partial R} \bar{\phi}_{g,i} V_i D_{g,i}^{sph}}, \quad (5)$$

where ∂R denotes the set of boundary reflector pin cells of region R, $\bar{\phi}_{g,i}$, V_i, and $D_{g,i}^{sph}$ are the average flux, volume, and SPH-corrected D of cell i, and $\gamma_{g,i}$ is the correction factor assigned to cell i.

The averaged factor $\bar{\gamma}_g$ is then applied to the SPH-corrected D of each reflector pin cell i, yielding the corrected reflector D in Eq. (6):

$$D_{g,i}^{\gamma} = \bar{\gamma}_g D_{g,i}^{sph} \quad . \quad (6)$$

Because the reflector configuration differs by type, a separate $\bar{\gamma}_g$ is evaluated for each reflector and applied accordingly, as summarized in Eq. (7):

$$D_{g,i}^{\gamma} = \begin{cases} \bar{\gamma}_g^{RE} D_{g,i}^{sph}, & i \in RE \\ \bar{\gamma}_g^{RC} D_{g,i}^{sph}, & i \in RC \\ \bar{\gamma}_g^{RX} D_{g,i}^{sph}, & i \in RX \end{cases} \quad . \quad (7)$$

3. Numerical results and analysis

3.1 Test problem

The proposed correction was first applied to a 2D SMR core loaded with 37 fuel assemblies. Four group PHGCs were generated with DeCART2D, and the pin-wise diffusion calculation was carried out with SPHINCS. The DeCART2D transport solution was taken as the reference, and only the power distribution was compared.

Fig. 5 shows the pin-wise and FA-wise power error distributions with the conventional SPH treatment and with the reflector D correction added. The correction reduces the pin-wise RMS error from 0.86 % to 0.73 % and the maximum error from 4.31 % to 3.61 %. At the assembly level, the RMS error falls from 0.51 % to 0.36 % and the maximum from 1.26 % to 0.81 %.

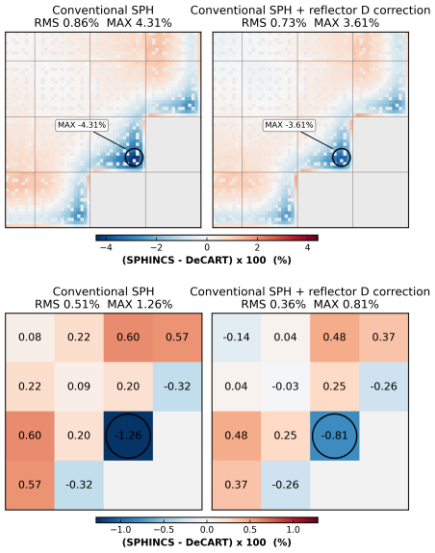


Fig. 5. Power error distributions for the 37-FA 2D core: pin-wise (top) and FA-wise (bottom), before (left) and after (right) the reflector *D* correction.

3.2 Application to 2D Whole-Core Problems

The same procedure was then applied to three 2D whole-core problems, summarized in Table I.

The APR1400 and OPR1000 cores use 16 × 16 FAs with several uranium enrichments and integral gadolinia (IGD) as the burnable absorber (BA), and both were analyzed at 500 ppm soluble boron under hot full power (HFP) with all rods out (ARO). The i-SMR core is designed for SBF operation and relies on CR for reactivity control, so both ARO and rodded configurations were considered at 0 ppm, and it employs HIGA [7] in addition to IGD.

In the rodded case, Ag–In–Cd CRs are inserted at eight assembly positions near the core center; since the problem is 2D, they are treated as fully inserted rather than at a partial insertion depth. All problems assume equilibrium xenon and transient samarium.

Table I. 2D core problems and their calculation conditions.

Problems	BA	Conditions
APR1400 2D	IGD	500 ppm, HFP, ARO Equilibrium Xe, transient Sm
OPR1000 2D	IGD	500 ppm, HFP, ARO Equilibrium Xe, transient Sm
i-SMR 2D	IGD, HIGA	0 ppm, HFP, ARO / Rodded Equilibrium Xe, transient Sm

The RE, RC, and RX reflector PHGCs were generated simultaneously from a single minicore calculation with 12 FAs. The PHGCs of the RE, RC, and RX nodes marked in red in Fig. 6 were then *D*-corrected and used in the core calculation.

SPHINCS was then run in three cases with the DeCART2D four-group PHGCs and compared against the DeCART2D reference. The cases differ only in the reflector treatment: SPH applied to the fuel only (SPH-F), to the fuel and reflector (SPH-F-R), and to both with the reflector *D* correction added (SPH-F-RD). SPH-F serves as a baseline, while the comparison between SPH-F-R and SPH-F-RD isolates the effect of the *D* correction.

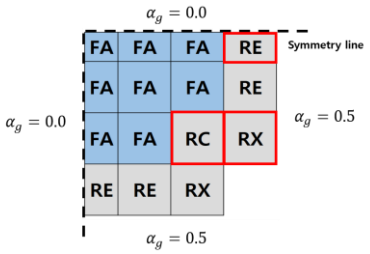


Fig. 6. Minicore problem for generating radial reflector PHGCs

Fig. 7 shows the pin- and FA-wise power error distributions for the APR1400 2D core at BOC. With SPH-F, the error forms a clear center-to-periphery tilt, and the pin-wise RMS reaches 3.56 % with a MAX of 7.25 %. SPH-F-R removes most of this tilt, lowering the RMS to 0.92 % and the MAX to 3.37 %.

Adding the reflector *D* correction, SPH-F-RD improves the result further, reducing the RMS to 0.62 % and the MAX to 2.75 %, with the reductions most evident near the core center. The FA-wise errors follow the same trend: the RMS decreases from 3.56 % to 0.91 % and then to 0.52 %, and the MAX from 5.96 % to 1.94 % and then to 1.32 %.

Fig. 8 compares the errors during depletion to check whether the correction remains effective. The hot pin power refers to the pins with a relative power above 1.0 in the DeCART2D solution, since the maximum relative error otherwise occurs in non-critical regions near the core periphery. SPH-F gives the largest errors, SPH-F-R reduces them substantially, and SPH-F-RD remains the most accurate, keeping the assembly RMS near 0.5 % with little variation with burnup. The correction therefore holds consistently over the whole burnup range.

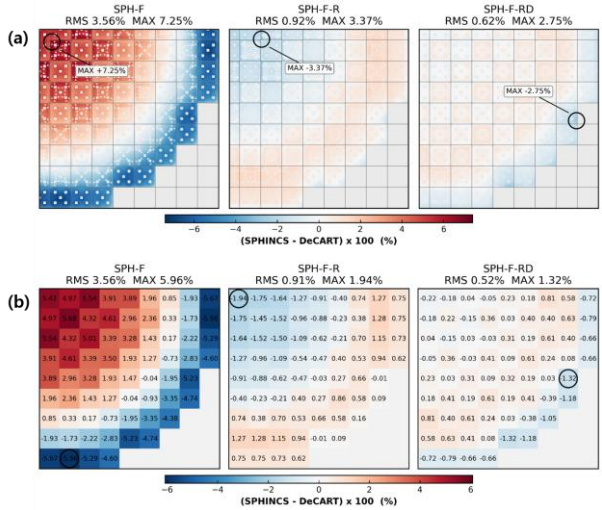


Fig. 7. Pin-wise (a) and FA-wise (b) power error distributions for the APR1400 2D core at BOC.

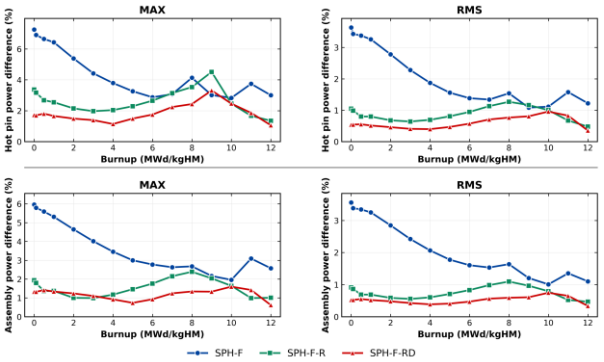


Fig. 8. MAX (left) and RMS (right) errors in the hot pin power (top) and the assembly power (bottom) during depletion for the APR1400 2D core.

The same trend appears in the OPR1000 core. As shown in Fig. 9, the pin-wise RMS error decreases from 2.65 % to 0.61 % with SPH-F-R and to 0.59 % with SPH-F-RD, and the assembly RMS from 2.66 % to 0.54 % and 0.46 %. Fig. 10 confirms that the improvement is maintained throughout depletion.

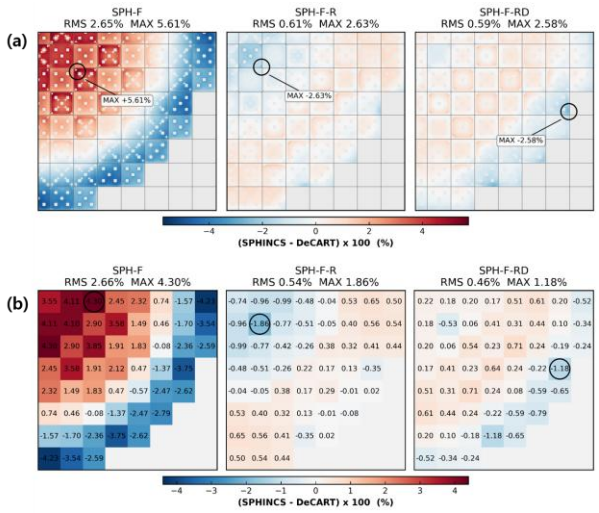


Fig. 9. Pin-wise (a) and FA-wise (b) power error distributions for the OPR1000 2D core at BOC.

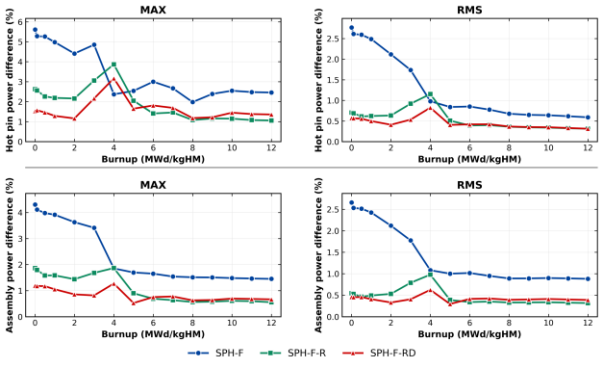


Fig. 10. MAX (left) and RMS (right) errors in the hot pin power (top) and the assembly power (bottom) during depletion for the OPR1000 2D core.

The i-SMR core in the ARO configuration also shows the same behavior. As shown in Fig. 11, the pin-wise RMS error decreases from 2.02 % to 0.87 % with SPH-F-R and to 0.78 % with SPH-F-RD, while the assembly RMS falls from 2.08 % to 0.74 % and 0.61 %. Fig. 12 shows that the improvement is retained up to 20 MWd/kgHM.

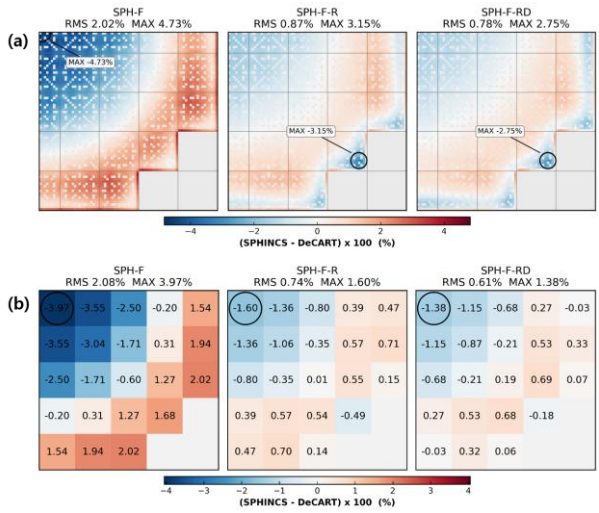


Fig. 11. Pin-wise (a) and FA-wise (b) power error distributions for the i-SMR 2D core (ARO) at BOC.

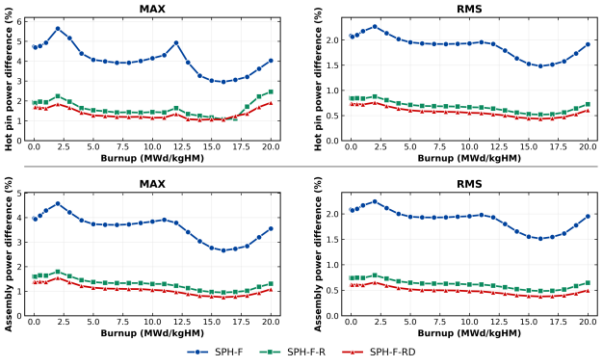


Fig. 12. MAX (left) and RMS (right) errors in the hot pin power (top) and assembly power (bottom) during depletion for the i-SMR 2D core (ARO).

The rodded problem was also evaluated to see whether the correction is still effective when the power is redistributed by CR insertion.

Fig. 13 shows the error distributions at BOC, where the red boxes mark the assemblies with the CRs fully inserted. As shown in Fig. 13, SPH-F leaves the largest error in the rodded region and its surroundings, with a pin-wise RMS of 1.62 % and an assembly RMS of 1.59 %. SPH-F-R lowers these to 0.93 % and 0.71 %, and SPH-F-RD to 0.87 % and 0.61 %, with the assembly MAX falling from 3.42 % to 1.74 %.

Fig. 14 shows that this holds throughout depletion, confirming that the correction remains effective under CR insertion.

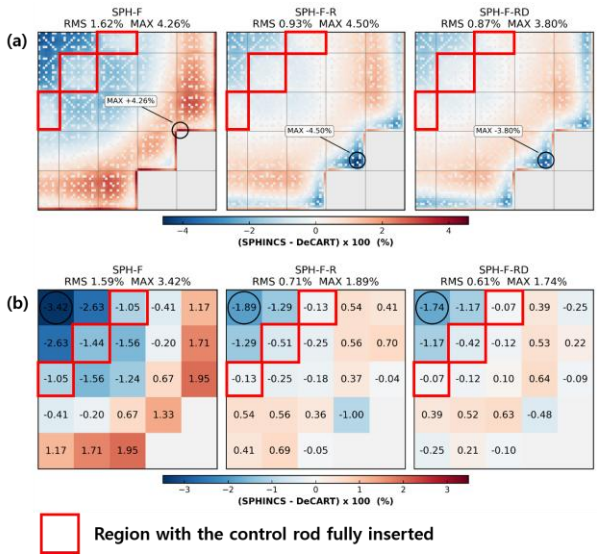


Fig. 13. Pin-wise (a) and FA-wise (b) power error distributions for the i-SMR 2D core (Rodded) at BOC.

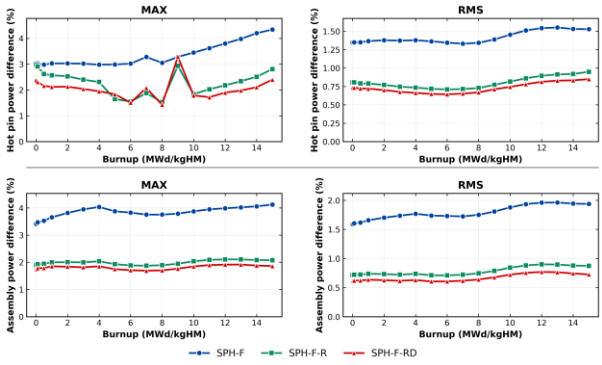


Fig. 14. MAX (left) and RMS (right) errors in the hot pin power (top) and assembly power (bottom) during depletion for the i-SMR 2D core (Rodded).

Future work will apply the method to 3D core calculations, where the axial reflector is treated in addition to the radial one, and assess it against MOC or Monte Carlo reference solutions.

4. Conclusions

A reflector D correction was proposed to reduce the residual power distribution error that remains after the SPH iteration in pin-wise core calculation. A factor γ multiplying the SPH-corrected reflector D was introduced and obtained in a closed form from the current-matching condition, with the D of FA kept fixed to preserve the two-step scheme. The correction is applied during the reflector PHGC generation and requires no change to the core solver.

The method was assessed for the APR1400, OPR1000, and i-SMR 2D cores against DeCART2D. Reflector SPH alone reduced the pin-wise RMS error to below 1 % in all cases, and the D correction lowered it further, with the improvement most evident near the core center. The same behavior was observed over the whole burnup range and under CR insertion.

Future work will apply the method to 3D core calculations, where the axial reflector is treated in addition to the radial one, and assess it comprehensively against 3D reference solutions.

ACKNOWLEDGEMENT

The authors would like to thank Dr. Cheon Bo Shim for helpful technical support throughout this work.
This work was supported by the Nuclear Safety Research Program through the Regulatory Research Management Agency for SMRs (RMAS) and the Nuclear Safety and Security Commission (NSSC) of the Republic of Korea (No. RS-2024-00509678).

REFERENCES

[1] Kang, H. O., Lee, B. J., & Lim, S. G. (2024). Light water SMR development status in Korea. *Nuclear Engineering and Design*, *419*, 112966.
[2] Hebert, A. (1993). A consistent technique for the pin-by-pin homogenization of a pressurized water reactor assembly. *Nuclear Science and Engineering*, *113*(3), 227-238.
[3] Yoon, J., Lee, H. C., Joo, H. G., & Kim, H. S. (2021). High performance 3D pin-by-pin neutron diffusion calculation based on 2D/1D decoupling method for accurate pin power estimation. *Nuclear Engineering and Technology*, *53*(11), 3543-3562.
[4] Lim, C., Kwon, S. J., & Yoon, J. (2025). Performance analysis of a two-step calculation procedure based on Monte Carlo and pin-wise diffusion methods for PWR core design. *Nuclear Engineering and Technology*, *57*(8), 103596.
[5] Cho, J. Y., Shim, C., Han, T. Y., Lee, K., Lee, C., Song, J. S., ... & Jo, C. K. (2016). DeCART2D v1. 1 user's manual. *KAERI/UM-40/2016*.
[6] Yoon, J., Lee, H. C., Joo, H. G., & Kim, H. S. (2021). High performance 3D pin-by-pin neutron diffusion calculation based on 2D/1D decoupling method for accurate pin power estimation. *Nuclear Engineering and Technology*, *53*(11), 3543-3562.
[7] Kim, J. S., Jung, T. S., & Yoon, J. (2024). Reactor core design with practical gadolinia burnable absorbers for soluble boron-free operation in the innovative SMR. *Nuclear Engineering and Technology*, *56*(8), 3144-3154.